

Recent advances on spinel-based protective coatings for solid oxide cell metallic interconnects produced by electrophoretic deposition

*Original*

Recent advances on spinel-based protective coatings for solid oxide cell metallic interconnects produced by electrophoretic deposition / Zanchi, E.; Sabato, A. G.; Molin, S.; Cempura, G.; Boccaccini, A. R.; Smeacetto, F.. - In: MATERIALS LETTERS. - ISSN 0167-577X. - ELETTRONICO. - 286:(2021), p. 129229. [10.1016/j.matlet.2020.129229]

*Availability:*

This version is available at: 11583/2870278 since: 2021-04-08T17:56:02Z

*Publisher:*

Elsevier B.V.

*Published*

DOI:10.1016/j.matlet.2020.129229

*Terms of use:*

This article is made available under terms and conditions as specified in the corresponding bibliographic description in the repository

*Publisher copyright*

(Article begins on next page)

# Recent advances on spinel-based protective coatings for solid oxide cell metallic interconnects produced by electrophoretic deposition

E. Zanchi<sup>1</sup>, A.G. Sabato<sup>2</sup>, S. Molin<sup>3</sup>, G. Cempura<sup>4</sup>, A.R. Boccaccini<sup>5</sup>, F. Smeacetto<sup>1</sup>

1. Department of Applied Science and Technology, Politecnico di Torino, Corso Duca degli Abruzzi 24, 10129 Torino, Italy

2. Institut de Recerca en Energia de Catalunya (IREC), Jardins de les Dones de Negre, 1, 2<sup>a</sup> pl., 08930 Sant Adrià de Besòs, Barcelona, Spain

3. Faculty of Electronics, Telecommunications and Informatics, Gdańsk University of Technology, ul. G. Narutowicza 11/12, 80-233 Gdańsk, Poland

4. AGH University of Science and Technology, al. Mickiewicza 30, 30-059, Krakow, Poland

5. Department of Materials Science and Engineering, University of Erlangen-Nuremberg, Cauerstr. 6, 91058 Erlangen, Germany

Corresponding author e-mail: [federico.smeacetto@polito.it](mailto:federico.smeacetto@polito.it)

**Keywords:** Electrophoretic deposition; Spinel coatings; Solid Oxide Cells.

## Abstract

The application of ceramic protective coatings to the metallic interconnects in solid oxide cells (SOC) is a viable and effective method to limit interconnect degradation issues. The aim of this featured letter is to present a critical overview of the main outcomes of current research on the use of the electrophoretic deposition (EPD) technique to produce protective coatings for SOC metallic interconnects, specifically focusing on different approaches to stabilise spinel-based suspensions, as well as the possible sintering procedures. The protective properties of EPD coatings are reviewed and discussed in terms of oxidation kinetics and area specific resistance evaluation.

## Introduction

Solid oxide cells (SOCs) are electrochemical energy conversion devices operating at temperatures in the range of 500-850 °C. The degradation of metallic interconnects is one of the main issues affecting the durability of SOC. Ceramic protective coatings are widely employed in order to reduce the chromium evaporation and the growth of the under laying oxide scale on metallic interconnect, which causes an undesired increase of the electrical resistance. The satisfactory performance of a protective coating is strictly related to its high electronic conductivity, thermal expansion coefficient and Cr and O<sub>2</sub>-blocking capability. Materials in the oxide spinel family have attracted attention thanks to their excellent balance between these characteristics in comparison with rare earth oxides and perovskites [1]. Among others,

manganese-cobalt and manganese-copper based oxide spinels have been reported to be favourable candidates for their high electronic conductivity at the typical SOCs operating temperatures ( $60\text{-}220\text{ S cm}^{-1}$ ) and compatible thermal expansion coefficients ( $10\text{-}12\ 10^{-6}\ \text{K}^{-1}$ ) with metallic materials typically used as interconnects [2]. The properties of these spinels can be adjusted by substituting part of the base elements by transition metals [3,4]. Spinel based coatings have been deposited by various methods, such as sputtering, screen printing, thermal spray, plasma spray, slurry deposition, dip coating and EPD [5,6]. EPD offers the possibility to deposit homogeneous layers in few seconds and at RT condition; moreover, the simple and adaptable setup makes EPD a suitable cost-effective technique for industrial applications. [7]. However, the engineering of the suspensions required for successful EPD, the optimization of the deposition parameters and the choice of appropriate sintering conditions is challenging, as they all contribute to the quality of the obtained coatings [8]. We intend to summarise recent developments on the use of EPD for the fabrication of spinel-based protective coatings for SOC interconnects and to highlight the advantages and challenges of EPD in such applications.

## 2. Electrophoretic deposition of spinel coatings

### 2.1 EPD of manganese-cobalt and manganese-copper spinel

Table 1 reports the EPD parameters for Mn-Co and Mn-Cu spinel-based coatings which have been applied in relevant studies published in the last five years.

Ref.	Year	Spinel Coating Material		Electrophoretic deposition					
		Composition	Synthesis method	Solution [vol%]	Iodine [g/l]	Solid load [g/l]	Voltage [V], time [s]	Electrodes distance [cm]	Substrate
[9]	2015	$\text{Mn}_{1.5}\text{Co}_{1.5}\text{O}_4$	Commercial	60 EtOH 40 H <sub>2</sub> O	-	37.5	5-50 V 5-120 s	-	Crofer 22 APU
[10]	2016	$\text{MnCo}_2\text{O}_4$	Commercial	100 EtOH	0.15	10.0	30-60 V 60-360 s	1	AISI 430
[11]	2017	$\text{Mn}_{1.5}\text{Co}_{1.5}\text{O}_4$	Commercial	60 EtOH 40 H <sub>2</sub> O	-	37.5	50 V 20s	1	Crofer 22 APU
[12,13]	2017	$\text{MnCo}_2\text{O}_4$ $\text{MnCo}_{1.7}\text{Fe}_{0.3}\text{O}_4$ $\text{MnCo}_{1.7}\text{Cu}_{0.3}\text{O}_4$	Spray pyrolysis	50 EtOH 50 IPA	-	39.4	35 V 40-100 s	1.5	Crofer 22 APU
[14]	2018	$\text{MnCo}_2\text{O}_4$	Commercial	50 EtOH 50 IPA	0.50	7.9	60 V 60 s	-	Crofer 22 APU
[15,16]	2018 2019	$\text{Mn}_{1.5}\text{Co}_{1.5}\text{O}_4$ $\text{Mn}_{1.43}\text{Co}_{1.43}\text{Cu}_{0.14}\text{O}_4$ $\text{Mn}_{1.35}\text{Co}_{1.35}\text{Cu}_{0.30}\text{O}_4$	Commercial $\text{Mn}_{1.5}\text{Co}_{1.5}\text{O}_4$ and CuO	60 EtOH 40 H <sub>2</sub> O	-	37.5	50 V 20 s	1	Crofer 22 APU

1 [17]	2019	Mn <sub>1.5</sub> Co <sub>1.5</sub> O <sub>4</sub> Mn <sub>1.45</sub> Co <sub>1.45</sub> Fe <sub>0.1</sub> O <sub>4</sub>	EDTA	80 Acet 20 IPA	0.50	10	60 V 30 s	1	Crofer 22 H
2									
3									
4 [18]	2019	Mn <sub>1.5</sub> Co <sub>1.5</sub> O <sub>4</sub>	Commercial	50 EtOH 50 IPA	0.50	15.8	60 V 60 s	-	Crofer 22 APU
5									
6									
7 [19,20]	2019 2020	Mn <sub>1.5</sub> Co <sub>1.5</sub> O <sub>4</sub> Mn <sub>1.43</sub> Co <sub>1.43</sub> Fe <sub>0.14</sub> O <sub>4</sub> Mn <sub>1.35</sub> Co <sub>1.35</sub> Fe <sub>0.30</sub> O <sub>4</sub>	Commercial Mn <sub>1.5</sub> Co <sub>1.5</sub> O <sub>4</sub> and Fe <sub>2</sub> O <sub>3</sub>	60 EtOH 40 H <sub>2</sub> O	-	37.5	50 V 20 s	1	Crofer 22 APU AISI 441
8									
9									
10									
11 [21]	2020	MnCo <sub>2</sub> O <sub>4</sub>	Commercial	50 EtOH 50 IPA	0.50	15.8	60 V 60 s	1.5	Crofer 22 H AISI 441 AISI430
12									
13									
14 [22]	2020	Mn <sub>1.4</sub> Co <sub>1.4</sub> Cu <sub>0.2</sub> O <sub>4</sub>	Commercial	50 IPA 50 ACAC	-	10	40-140 V 2-10 min	-	SUS430
15									
16									
17 [23]	2017	Cu <sub>1.3</sub> Mn <sub>1.7</sub> O <sub>4</sub>	GNP	75 ACE 25 EtOH	1.09	9	20 V 10 min	1.5	Crofer 22 APU
18									
19 [24,25]	2018	CuMn <sub>1.8</sub> O <sub>4</sub>	GNP	75 ACE 25 EtOH	1.09	9	20 V 10 min	-	Crofer 22 APU Crofer 22 H
20									
21									
22 [26]	2019	CuMn <sub>1.8</sub> O <sub>4</sub> Cu <sub>0.6</sub> Ni <sub>0.4</sub> Mn <sub>2</sub> O <sub>4</sub>	GNP	75 ACE 25 EtOH	1.09	9	20 V 10 min	-	Crofer 22 APU
23									
24									
25									

Table 1: Summary of materials and experimental parameters for the electrophoretic deposition of Mn-Co and Mn-Cu spinel-based coatings for SOC metallic interconnects.

Most of the studies on EPD deposition of spinel coatings have focused on manganese-cobalt spinel. The solvent for preparation of EPD suspension can be composed of fully organic liquids or partially aqueous solutions. In the first case, the addition of a surface charge enhancer (i.e. I<sub>2</sub>) is generally necessary to stabilize the suspension [10,14,17,18,21]. When I<sub>2</sub> is not employed with organic solvents, a stable suspension is made by significantly increasing the particles load [12,13]. A possible explanation is that when the concentration of solid particles is higher, the electrostatic interactions between particles could have a stabilizing effect toward the suspensions, avoiding their sedimentation. Replacing a certain amount of organic solvent with water is an eco-friendly solution and does not require the addition of surface charger, due to the presence of sufficient free ions. A possible risk related to the use of water is the development of gas at the electrodes causing a non-homogeneous deposition [7]; however, it is widely reported that an optimal deposition of Mn-Co spinel coating can occur by applying up to 50 V [9,11,15,16,19,20]. The applied voltage can be higher in the case the solvents are fully organic.

The EPD process typically allows to obtain 10 to 20 μm coatings; this range of thickness is believed to be suitable to act as physical barrier against Cr evaporation and O<sub>2</sub> inward diffusion. Molin et al. [11] demonstrated the importance to obtain a coating thick enough to limit these phenomena, the EPD Mn-Co coating was more protective than the thin (1-1.5 μm) coatings obtained by both sputtering and thermal co-evaporation method. Although EPD is known to be less influenced by the line-of-sight compared to other

1 techniques, depositions are generally performed on flat coupons in most of the studies. However, the  
2 typical design of metallic interconnects employed in SOC stacks exhibits complex shapes and channelled  
3 surfaces. To this purpose, Talic et al. [18] recently demonstrated the uniformity of EPD spinel coatings  
4 obtained on a channelled sample of Crofer22APU and on a mesh of Crofer22H. Recently Mn-Cu spinels are  
5 receiving increasing attention due to environmental and economic advantages compared to cobalt  
6 containing coatings. Furthermore they possess a higher electronic conductivity (up to 100-220 S cm<sup>-1</sup>,  
7 depending on the exact Mn/Cu ratio) than Mn-Co based spinels, together with a CTE highly compatible with  
8 Crofer22APU [2]. However, few studies have reported the electrophoretic deposition of Cu-Mn spinel  
9 coatings [23–26]; EPD parameters are reported in  
10 Table 1. Despite the fact that Mn-Cu spinel-based systems are theoretically more suitable than Mn-Co  
11 based ones, to the authors best knowledge, there is a lack in long term tests (>2000h) of these coatings: i.e.  
12 the effect of long terms exposure to high temperatures on the Cu volatility still needs to be evaluated.  
13  
14  
15  
16  
17  
18  
19  
20  
21  
22  
23  
24

## 25 **2.2 EPD of copper and iron doped manganese-cobalt spinel**

26 Modifications of the chemical composition of the parent spinel have been identified as an effective strategy  
27 to improve the behaviour of Mn-Co spinel, i.e. tuning its CTE, electrical conductivity or sinterability [3,4].  
28 The substitution of a certain percentage of the base spinel elements by transition metals is generally  
29 referred as “doping”. The most common dopant elements considered are Fe and Cu; substituted coatings  
30 were produced following “ex-situ” or “in-situ” doping approaches.  
31  
32

33 In the ex-situ approach the modified spinel is synthesized before the coating deposition, employing similar  
34 techniques to those of the undoped Mn-Co spinel. For example, Talic et al. [4,12,13] reported on the use of  
35 spray pyrolysis to synthesize both undoped and iron or copper doped Mn-Co spinel; Bednarz et al. [17] used  
36 a EDTA gel processes instead. In this case, the deposition occurs on the cathode as for the unmodified  
37 spinel, as shown in Figure 2 A.  
38  
39

40 The in-situ doping consists in the co-deposition of the desired amount of the oxide of the additional  
41 element (Fe<sub>2</sub>O<sub>3</sub>, CuO etc.) and of the base spinel (e.g. Mn<sub>1.5</sub>Co<sub>1.5</sub>O<sub>4</sub>). In this case, the homogeneous  
42 deposition of the precursors depends on the optimization of the suspension, whereas the subsequent  
43 sintering treatment allows the additional element to enter the spinel structure. Sabato et al. [16] co-  
44 deposited commercial Mn<sub>1.5</sub>Co<sub>1.5</sub>O<sub>4</sub> (d<sub>50</sub>=634 nm) and CuO (d<sub>50</sub>=526 nm) producing coatings with different  
45 levels of copper doping. Zeta potential measurements showed that both precursors developed a positive  
46 surface charge in the selected liquid medium (+13 mV and +6mV respectively), thus leading to cathodic  
47 deposition (see Figure 2 B). Zanchi et al. [19,20] produced coatings doped with different amount of iron by  
48 co-depositing Mn<sub>1.5</sub>Co<sub>1.5</sub>O<sub>4</sub> (d<sub>50</sub>=634 nm) and Fe<sub>2</sub>O<sub>3</sub> (d<sub>50</sub>=75 nm). In this case, iron oxide develops a negative  
49 surface charge (-9.9 mV); however, a fully cathodic deposition occurred. Indeed, the electrostatic  
50  
51  
52  
53  
54  
55  
56  
57  
58  
59  
60  
61  
62  
63  
64  
65

interactions between opposite charges, the smaller dimension of  $\text{Fe}_2\text{O}_3$  particles and the low concentration of  $\text{Fe}_2\text{O}_3$  used led to the co-deposition mechanism schematized in Figure 2 C.

The co-deposition approach proposed is a new and an interesting route, since the improvement of the in-situ doping could allow to produce multi-layered and multi substituted coatings or with a composition gradient, by simply varying the precursors' concentration in the EPD suspension.

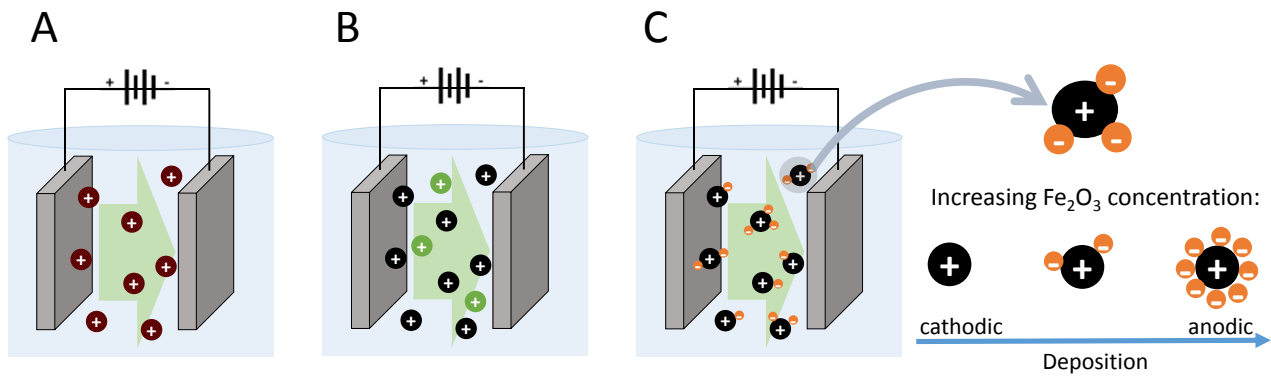


Figure 1: Schematic diagram showing the electrophoretic deposition process of manganese-cobalt spinel-based coatings. A) ex-situ doped spinel; B) in-situ copper doping; C) in-situ iron doping.

### 3. Evaluation of the sintering parameters

An optimized EPD process allows to deposit homogeneous layers of packed ceramic particles; however, an appropriate sintering treatment is always required in order to obtain a well densified protective coating. The choice of the treatment parameters is crucial: temperature, time and atmosphere of the sintering process should be balanced between the need to obtain a high degree of reaction of the deposited particles and the necessity to avoid the excessive oxidation of the under laying steel substrate.

Achieving a high densification of the coatings is essential to guarantee an effective barrier behaviour. Indeed, any residual open porosity which constitutes a preferential route for Cr evaporation and oxygen inward migration (Figure 2A) must be avoided, in favour of the formation of a densified coating layer close to the oxide scale and preferably close porosity (Figure 2B) [13].

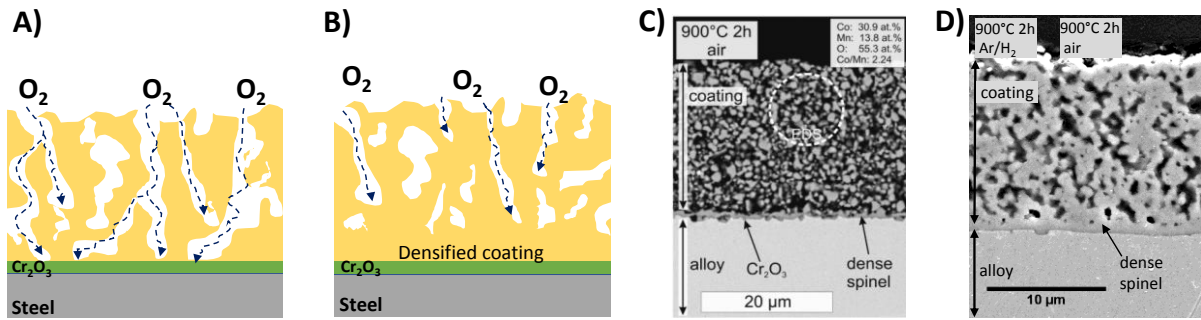


Figure 2: Schematic diagram of EPD coatings: A) sintered non-protective, B) sintered protective coating. C) SEM cross-section view of Mn-Co spinel sintered at 900°C, 2h in air, adapted from [14]; D) SEM cross-section view of Mn-Co spinel sintered at 1000°C, 2h in Ar/H<sub>2</sub> and at 900°C, 2h in air. Please note the different magnification of the images.

The sintering parameters selected in the discussed studies are summarized in Table 2. A first possibility is to submit the Mn-Co spinel coating to a heat treatment (i.e. 800-900 °C) in oxidizing condition. Nevertheless, the coating densification reached by an oxidizing treatment is generally poor (Figure 2C), unless the heat treatment is performed at very high temperature (i.e. 1100 °C) [14].

It is possible to assert that a two-step sintering approach (consisting of a first heat treatment in reducing atmosphere followed by a second one in oxidising conditions) is widely recognized as a more effective post-deposition treatment for spinel based protective coatings deposited by EPD. In the case of in-situ doped coatings, the two-step sintering is always required and it is normally referred as “reactive sintering”. During the reducing step the Mn-Co spinel transform into MnO and Co; in addition, both copper and iron doped coatings form respectively metallic Cu [15,16,22] and Co-Fe intermetallic phase [19]. The re-oxidation treatment allows both the re-formation of the cubic and/or tetragonal phase of the spinel and the introduction of the dopant element; both iron and copper doping are reported to stabilize the cubic structure of Mn-Co spinel [15,16,19]. Thanks to the reduction step, the densification of Mn-Co coating obtained at 900 °C is definitely higher compared to the one-step sintering [14], as shown in Figure 2 C and D. Moreover, the re-oxidation step could easily be performed during the stack consolidation, also considering that the coating in the reduced state is easier to handle than the as-deposited coating.

The two-step sintering procedure can be applied to manganese copper spinel too. In ref. [23] uniaxial pressure was also applied before each heat treatment in order to achieve a sufficient densification; this procedure was then substituted by optimizing the reducing heat treatment (1000°C for 12-24 h) [24–26].

REF	Sintering parameters			
	Type	Temperature [°C]	Time [h]	Atmosphere
[9]	Oxidizing	800, 1000, 1100	2	Static air
[10]	Oxidizing	1050	1	Static air
[11]	Oxidizing	1000	2	Static air
[12]	Two-step	- 900	2	N <sub>2</sub> /H <sub>2</sub> (9 vol.%)
		- 800	2	Static air
[13]	Oxidizing	900	2	Static air
	Two-step	- 900, 1100	2 - 5	N <sub>2</sub> /H <sub>2</sub> (9 vol.%)
[14]	Two-step	- 800	2 - 5	Static air
		Oxidizing	900, 1000, 1100	2
[15,16]	Two-step	- 900, 1000, 1100	2	Ar/H <sub>2</sub> (9 vol.%)
		- 900	2	Static air
[17]	Two-step	- 900	2	Ar/H <sub>2</sub> (4 vol.%)
		- 900	2	Static air
[19,20]	Two-step	- 900	2	Ar/H <sub>2</sub> (9 vol.%)
		- 900	4	Static air
[21]	Oxidizing	- 900, 1000	2	Ar/H <sub>2</sub> (4 vol.%)
		- 900	2	Static air
[22]	Two-step	900	2	Static air
		800	4	Static air
[23]	Two-step	-800	2	Ar/H <sub>2</sub> (5 vol.%)
		-750	2	Static air
Manganese copper spinel	Two-step	-850*	1	Ar/H <sub>2</sub> (2 vol.%)
		-850*	100	Static air
		-1000	12 - 24	Ar/H <sub>2</sub> (2 vol.%)
[24-26]	Two-step	-850	100	Static air

\*Uniaxial pressure (from 10 to 100ksi) was applied before the heat treatment

Table 2: sintering parameters for spinel-based coatings after EPD.

#### 4. Evaluation of the coating properties

The protective properties of coatings for metallic interconnects can be evaluated by the improvement of the oxidation resistance based on thermogravimetric measurements and the area specific resistance (ASR), as well as the Cr evaporation/migration.

Many studies report that spinel-based coatings exhibit parabolic oxidation, reducing the oxidation rate constant ( $k_p$ ) of the steel substrate; the positive effect of the spinel coatings is generally more prominent at higher aging temperatures. Talic et al. [12] reported that  $k_p$  of pre-oxidized Crofer 22 APU at 900°C is one order of magnitude higher than for coated samples; in this case, all undoped, Cu or Fe-doped MnCo<sub>2</sub>O<sub>4</sub> spinel coatings obtained by EPD showed no remarkable difference. The same coatings brought less significant improvement on the oxidation resistance at 800°C and 700°C.



1  
2  
3  
4  
5  
6  
7  
8  
9  
10  
11  
12  
13  
14  
15  
16  
17  
18  
19  
20  
21  
22  
23  
24  
25  
26  
27  
28  
29  
30  
31  
32  
33  
34  
35  
36  
37  
38  
39  
40  
41  
42  
43  
44  
45  
46  
47  
48  
49  
50  
51  
52  
53  
54  
55  
56  
57  
58  
59  
60  
61  
62  
63  
64  
65

However, the joint choice of the steel substrate/coating composition, as well as the evaluation of optimal processing parameters play a major role especially at lower aging temperature. To this purpose, Zanchi et al. [19] found that the oxidation rate of Crofer 22 APU at 750°C is halved by  $Mn_{1.5}Co_{1.5}O_4$  coating and reduced by one order of magnitude when a Fe-doped  $Mn_{1.5}Co_{1.5}O_4$  spinel coating is applied by EPD and the sintering procedure is optimized. Indeed, the adjustment of the sintering parameters leads to a higher densification of the Fe-doped coating, whose positive influence is confirmed for oxidation tests at 800°C as well [13]. Bednarz et al. [17] studied the oxidation performance of Crofer 22 H, assessing that undoped and Fe-doped  $Mn_{1.5}Co_{1.5}O_4$  sequentially reduce the  $k_p$  at both 750 and 800 °C. Talic et al. [21] confirmed similar results for Crofer 22 H coated with  $MnCo_2O_4$ , whereas the performance of cheaper steels, like AISI 441 and AISI 430, does not seem to improve with the same coating compared to the bare substrates.

The measure of ASR can be in continuous (i.e. continuously recorded on samples at high temperature) or discontinuous oxidation (i.e. measures on pre-oxidised samples) and using different contact materials, e.g. Pt or lanthanum strontium manganite (LSM). The choice of the test method affects the reactions at the interfaces and the determination of the real contact area, thus leading to marked mismatch between the final values. The graph in Figure 3 A presents ASR data (dots) together with aging time (columns) of relevant studies on EPD deposited spinel coatings with various compositions at both 800 and 750°C on different interconnects; when not specified, the reported results are obtained in continuous oxidation and using LSM contacts. It is apparent from this graph that the ASR values from discontinuous measurements with Pt contacts reported in ref. [17] differ significantly from all the other studies; in this case, the high ASR is not due to the uncontrolled growth of the oxide scale, but likely to a poor reaction between coating and contact material, with a consequent overestimation of the real contact area.

The comparison of all reported studies on Crofer 22 APU obtained in continuous oxidation at 800°C reveals that the coating composition has a minor influence on the long-term conductivity. Indeed, Sabato et al. [16] reported only a slightly lower ASR of Cu-doped  $Mn_{1.5}Co_{1.5}O_4$ , but for Talic et al. [12] copper doping of  $MnCo_2O_4$  did not bring any advantage. ASR measured at 750 °C for both coated Crofer 22 APU and AISI 441 in [20] was moderately higher than at 800°C, in line with the semiconductor-type behaviour (thermally activated electronic conduction) of the spinel coating. Moreover, the final ASR values of both Crofer 22 APU and AISI 441 coated with the same coatings appear completely comparable after 3200 h at 750°C; this suggests that at this temperature the use of low-cost interconnects coupled with effective coatings is definitely convenient. Indeed, Crofer 22 APU is reported to develop the so called “reaction layer” (showed in Figure 3 B), causing the progressive increase of the area specific resistance [20]. However, few studies have investigated ASR of EPD spinel coatings on cheap steel substrates, suitable for intermediate temperature SOCs.

To summarize, the values of  $k_p$  and ASR strictly depend on the choice of the testing apparatus and the chosen parameters. For this reason, the comparison of the results from different studies is complex and further research needs to examine more closely the links between the deposition methods and the influence on the final performances of the coatings. For example, Molin et al. [11] assessed that the EPD coating on Crofer 22 APU developed a lower ASR (800°C) than the same spinel coating deposited by sputtering and thermal co-evaporation. On the other hand, various (Mn,Co)3O4 spinel coatings deposited by sol-gel dip-coating on AISI 430 exhibited an ASR between 11-15 mΩ cm<sup>2</sup> after 1000 h at 800°C [27]; however, Chen et al. [28] obtained a Co-Mn-O spinel coating by a double growth plasma alloying process on AISI 430 and measured an ASR value of 29 mΩ cm<sup>2</sup> (continuous oxidation with Pt contacts) after 408 h at 800°C. Finally, MnCo<sub>2</sub>O<sub>4</sub> and MnCo<sub>1.8</sub>Fe<sub>0.2</sub>O<sub>4</sub> coatings on Crofer 22 APU prepared by a two-step impregnation method described in ref. [29] showed an ASR of around 15 mΩ cm<sup>2</sup> after 5000h at 750°C (LSM contacts).

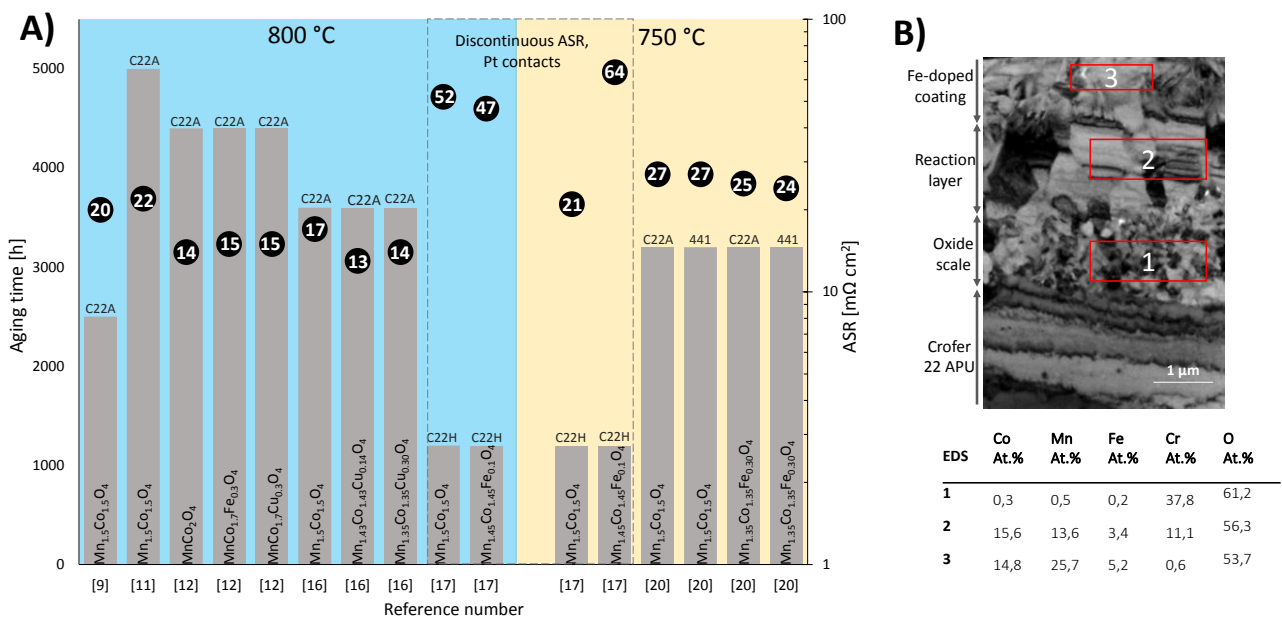


Figure 3: A) Long-term ASR values (dots) with relative aging time (columns) of relevant studies of EPD coatings. Both the coating compositions and the steels substrates are reported on the graph. B) TEM overview of a FIB lamella showing the interface developed between Crofer 22 APU and Fe-doped Mn<sub>1.5</sub>Co<sub>1.5</sub>O<sub>4</sub> coating after 3200 h at 750 °C.

## 5. Future perspectives and concluding remarks

All studies reviewed here support the statement that EPD is effective as a versatile deposition method for SOCs protective coating applications. Together these studies provide important insights into the crucial role

1 played by ceramic coatings in solid oxide cells durability and performance. These findings have significant  
2 implications for the understanding of how EPD can be used to design and process new spinel compositions,  
3 especially taking advantage of a two-step sintering process. Enhanced efficiency in electrochemical energy  
4 conversion can be achieved only by suitable material choice with proper functional requirements.  
5

6  
7 Several aspects of EPD process upscaling for coating large parts remain as future challenges about which  
8 relatively little is known. The processing and testing of real dimension plates coated by EPD and tested in a  
9 SOC stack is, therefore, an essential next step in confirming EPD as a viable process for spinel-based  
10 protective coatings in SOC technologies.  
11  
12  
13

## 14 **Acknowledgments**

15  
16  
17  
18 F. S. and A. R. B. would like to acknowledge the KMM-VIN (<http://www.kmm-vin.eu/home/fellowships>) 11<sup>th</sup>  
19 call granted to E. Zanchi. This project has received funding from the European Union's Horizon 2020  
20 research and innovation programme under grant agreement No 823717 – ESTEEM3.  
21  
22  
23  
24  
25  
26  
27

## 28 **References**

- 29  
30  
31 [1] J.C.W. Mah, A. Muchtar, M.R. Somalu, M.J. Ghazali, Metallic interconnects for solid oxide fuel cell:  
32 A review on protective coating and deposition techniques, *Int. J. Hydrogen Energy*. 42 (2017) 9219–9229.  
33 <https://doi.org/10.1016/j.ijhydene.2016.03.195>.  
34  
35  
36  
37 [2] A. Petric, H. Ling, Electrical conductivity and thermal expansion of spinels at elevated temperatures,  
38 *J. Am. Ceram. Soc.* 90 (2007) 1515–1520. <https://doi.org/10.1111/j.1551-2916.2007.01522.x>.  
39  
40  
41 [3] A. Masi, M. Bellusci, S.J. McPhail, F. Padella, P. Reale, J.-E. Hong, R. Steinberger-Wilckens, M. Carlini,  
42 The effect of chemical composition on high temperature behaviour of Fe and Cu doped Mn-Co spinels,  
43 *Ceram. Int.* 43 (2016) 2829–2835. <https://doi.org/10.1016/j.ceramint.2016.11.135>.  
44  
45  
46  
47 [4] B. Talic, P.V. Hendriksen, K. Wiik, H.L. Lein, Thermal expansion and electrical conductivity of Fe and  
48 Cu doped MnCo<sub>2</sub>O<sub>4</sub> spinel, *Solid State Ionics*. 326 (2018) 90–99. <https://doi.org/10.1016/j.ssi.2018.09.018>.  
49  
50  
51  
52 [5] K.H. Tan, H.A. Rahman, H. Taib, Coating layer and influence of transition metal for ferritic stainless  
53 steel interconnector solid oxide fuel cell: A review, *Int. J. Hydrogen Energy*. 44 (2019) 30591–30605.  
54 <https://doi.org/10.1016/j.ijhydene.2019.06.155>.  
55  
56  
57  
58 [6] N. Shaigan, W. Qu, D.G. Ivey, W. Chen, A review of recent progress in coatings, surface  
59 modifications and alloy developments for solid oxide fuel cell ferritic stainless steel interconnects, *J. Power*  
60 *Sources*. 195 (2010) 1529–1542. <https://doi.org/10.1016/j.jpowsour.2009.09.069>.  
61  
62  
63  
64  
65

- 1  
2  
3  
4  
5  
6  
7  
8  
9  
10  
11  
12  
13  
14  
15  
16  
17  
18  
19  
20  
21  
22  
23  
24  
25  
26  
27  
28  
29  
30  
31  
32  
33  
34  
35  
36  
37  
38  
39  
40  
41  
42  
43  
44  
45  
46  
47  
48  
49  
50  
51  
52  
53  
54  
55  
56  
57  
58  
59  
60  
61  
62  
63  
64  
65
- [7] L. Besra, M. Liu, A review on fundamentals and applications of electrophoretic deposition (EPD), *Prog. Mater. Sci.* 52 (2007) 1–61. <https://doi.org/10.1016/j.pmatsci.2006.07.001>.
- [8] H. Abdoli, S. Molin, H. Farnoush, Effect of interconnect coating procedure on solid oxide fuel cell performance, *Mater. Lett.* 259 (2020) 126898. <https://doi.org/10.1016/j.matlet.2019.126898>.
- [9] F. Smeacetto, A. De Miranda, S. Cabanas Polo, S. Molin, D. Boccaccini, M. Salvo, A.R. Boccaccini, Electrophoretic deposition of Mn<sub>1.5</sub>Co<sub>1.5</sub>O<sub>4</sub> on metallic interconnect and interaction with glass-ceramic sealant for solid oxide fuel cells application, *J. Power Sources.* 280 (2015) 379–386. <https://doi.org/10.1016/j.jpowsour.2015.01.120>.
- [10] M. Mirzaei, A. Simchi, M.A. Faghihi-Sani, A. Yazdanyar, Electrophoretic deposition and sintering of a nanostructured manganese-cobalt spinel coating for solid oxide fuel cell interconnects, *Ceram. Int.* 42 (2016) 6648–6656. <https://doi.org/10.1016/j.ceramint.2016.01.012>.
- [11] S. Molin, A.G. Sabato, M. Bindi, P. Leone, G. Cempura, M. Salvo, S. Cabanas Polo, A.R. Boccaccini, F. Smeacetto, Microstructural and electrical characterization of Mn-Co spinel protective coatings for solid oxide cell interconnects, *J. Eur. Ceram. Soc.* 37 (2017) 4781–4791. <https://doi.org/10.1016/j.jeurceramsoc.2017.07.011>.
- [12] B. Talic, S. Molin, K. Wiik, P.V. Hendriksen, H.L. Lein, Comparison of iron and copper doped manganese cobalt spinel oxides as protective coatings for solid oxide fuel cell interconnects, *J. Power Sources.* 372 (2017) 145–156. <https://doi.org/10.1016/j.jpowsour.2017.10.060>.
- [13] B. Talic, H. Falk-Windisch, V. Venkatachalam, P.V. Hendriksen, K. Wiik, H.L. Lein, Effect of coating density on oxidation resistance and Cr vaporization from solid oxide fuel cell interconnects, *J. Power Sources.* 354 (2017) 57–67. <https://doi.org/10.1016/j.jpowsour.2017.04.023>.
- [14] M. Bobruk, S. Molin, M. Chen, T. Brylewski, P.V. Hendriksen, Sintering of MnCo<sub>2</sub>O<sub>4</sub> coatings prepared by electrophoretic deposition, *Mater. Lett.* 213 (2018) 394–398. <https://doi.org/10.1016/j.matlet.2017.12.046>.
- [15] S. Molin, A.G. Sabato, H. Javed, G. Cempura, A.R. Boccaccini, F. Smeacetto, Co-deposition of CuO and Mn<sub>1.5</sub>Co<sub>1.5</sub>O<sub>4</sub> powders on Crofer22APU by electrophoretic method: Structural, compositional modifications and corrosion properties, *Mater. Lett.* 218 (2018) 329–333. <https://doi.org/10.1016/j.matlet.2018.02.037>.
- [16] A.G. Sabato, S. Molin, H. Javed, E. Zanchi, A.R. Boccaccini, F. Smeacetto, In-situ Cu-doped MnCo-spinel coatings for solid oxide cell interconnects processed by electrophoretic deposition, *Ceram. Int.* 45 (2019) 19148–19157. <https://doi.org/10.1016/j.ceramint.2019.06.161>.

- 1  
2  
3  
4  
5  
6  
7  
8  
9  
10  
11  
12  
13  
14  
15  
16  
17  
18  
19  
20  
21  
22  
23  
24  
25  
26  
27  
28  
29  
30  
31  
32  
33  
34  
35  
36  
37  
38  
39  
40  
41  
42  
43  
44  
45  
46  
47  
48  
49  
50  
51  
52  
53  
54  
55  
56  
57  
58  
59  
60  
61  
62  
63  
64  
65
- [17] M. Bednarz, S. Molin, M. Bobruk, M. Stygar, E. Długoń, M. Sitarz, T. Brylewski, High-temperature oxidation of the Crofer 22 H ferritic steel with Mn<sub>1.45</sub>Co<sub>1.45</sub>Fe<sub>0.104</sub> and Mn<sub>1.5</sub>Co<sub>1.5</sub>O<sub>4</sub> spinel coatings under thermal cycling conditions and its properties, *Mater. Chem. Phys.* 225 (2019) 227–238. <https://doi.org/10.1016/j.matchemphys.2018.12.090>.
- [18] B. Talic, A.C. Wulff, S. Molin, K.B. Andersen, P. Zielke, H.L. Frandsen, Investigation of electrophoretic deposition as a method for coating complex shaped steel parts in solid oxide cell stacks, *Surf. Coatings Technol.* 380 (2019) 1–8. <https://doi.org/10.1016/j.surfcoat.2019.125093>.
- [19] E. Zanchi, B. Talic, A.G. Sabato, S. Molin, A.R. Boccaccini, F. Smeacetto, Electrophoretic co-deposition of Fe<sub>2</sub>O<sub>3</sub> and Mn<sub>1.5</sub>Co<sub>1.5</sub>O<sub>4</sub>: Processing and oxidation performance of Fe-doped Mn-Co coatings for solid oxide cell interconnects, *J. Eur. Ceram. Soc.* 39 (2019) 3768–3777. <https://doi.org/10.1016/j.jeurceramsoc.2019.05.024>.
- [20] E. Zanchi, S. Molin, A.G. Sabato, B. Talic, G. Cempura, A.R. Boccaccini, F. Smeacetto, Iron doped manganese cobaltite spinel coatings produced by electrophoretic co-deposition on interconnects for solid oxide cells: Microstructural and electrical characterization, *J. Power Sources.* 455 (2020) 227910. <https://doi.org/10.1016/j.jpowsour.2020.227910>.
- [21] B. Talic, V. Venkatachalam, P.V. Hendriksen, R. Kiebach, Comparison of MnCo<sub>2</sub>O<sub>4</sub> coated Crofer 22 H, 441, 430 as interconnects for intermediate-temperature solid oxide fuel cell stacks, *J. Alloys Compd.* 821 (2020) 153229. <https://doi.org/10.1016/j.jallcom.2019.153229>.
- [22] I. Aznam, J.C.W. Mah, A. Muchtar, M.R. Somalu, M.J. Ghazali, Electrophoretic deposition of (Cu,Mn,Co)<sub>3</sub>O<sub>4</sub> spinel coating on SUS430 ferritic stainless steel: Process and performance evaluation for solid oxide fuel cell interconnect applications, *J. Eur. Ceram. Soc.* (2020). <https://doi.org/10.1016/j.jeurceramsoc.2020.09.074>.
- [23] Z. Sun, S. Gopalan, U.B. Pal, S.N. Basu, Cu<sub>1.3</sub>Mn<sub>1.7</sub>O<sub>4</sub> spinel coatings deposited by electrophoretic deposition on Crofer 22 APU substrates for solid oxide fuel cell applications, *Surf. Coatings Technol.* 323 (2017) 49–57. <https://doi.org/10.1016/j.surfcoat.2016.09.028>.
- [24] Z. Sun, R. Wang, A.Y. Nikiforov, S. Gopalan, U.B. Pal, S.N. Basu, CuMn<sub>1.8</sub>O<sub>4</sub> protective coatings on metallic interconnects for prevention of Cr-poisoning in solid oxide fuel cells, *J. Power Sources.* 378 (2018) 125–133. <https://doi.org/10.1016/j.jpowsour.2017.12.031>.
- [25] R. Wang, Z. Sun, U.B. Pal, S. Gopalan, S.N. Basu, Mitigation of chromium poisoning of cathodes in solid oxide fuel cells employing CuMn<sub>1.8</sub>O<sub>4</sub> spinel coating on metallic interconnect, *J. Power Sources.* 376 (2018) 100–110. <https://doi.org/10.1016/j.jpowsour.2017.11.069>.

1 [26] Z. Sun, S.G.B.P.N. Basu, Electrophoretically Deposited Copper Manganese Spinel Coatings for  
2 Prevention of Chromium Poisoning in Solid Oxide Fuel Cells, in: *Energy Technol.*, 2019: pp. 265–272.  
3 [https://link.springer.com/chapter/10.1007%2F978-3-030-06209-5\\_27](https://link.springer.com/chapter/10.1007%2F978-3-030-06209-5_27).  
4

5 [27] Z. Shen, J. Rong, X. Yu,  $Mn_xCo_{3-x}O_4$  spinel coatings: Controlled synthesis and high temperature  
6 oxidation resistance behavior, *Ceram. Int.* 46 (2020) 5821–5827.  
7 <https://doi.org/10.1016/j.ceramint.2019.11.032>.  
8  
9

10 [28] F. Cheng, J. Sun, Fabrication of a double-layered Co-Mn-O spinel coating on stainless steel via the  
11 double glow plasma alloying process and preoxidation treatment as SOFC interconnect, *Int. J. Hydrogen*  
12 *Energy*. 44 (2019) 18415–18424. <https://doi.org/10.1016/j.ijhydene.2019.05.060>.  
13  
14  
15

16 [29] S. Molin, P. Jasinski, L. Mikkelsen, W. Zhang, M. Chen, P. V. Hendriksen, Low temperature  
17 processed  $MnCo_2O_4$  and  $MnCo_{1.8}Fe_{0.2}O_4$  as effective protective coatings for solid oxide fuel cell  
18 interconnects at 750 °C, *J. Power Sources*. 336 (2016) 408–418.  
19  
20  
21  
22  
23 <https://doi.org/10.1016/j.jpowsour.2016.11.011>.  
24  
25  
26  
27  
28  
29  
30  
31  
32  
33  
34  
35  
36  
37  
38  
39  
40  
41  
42  
43  
44  
45  
46  
47  
48  
49  
50  
51  
52  
53  
54  
55  
56  
57  
58  
59  
60  
61  
62  
63  
64  
65

Figure 1  
[Click here to download high resolution image](#)

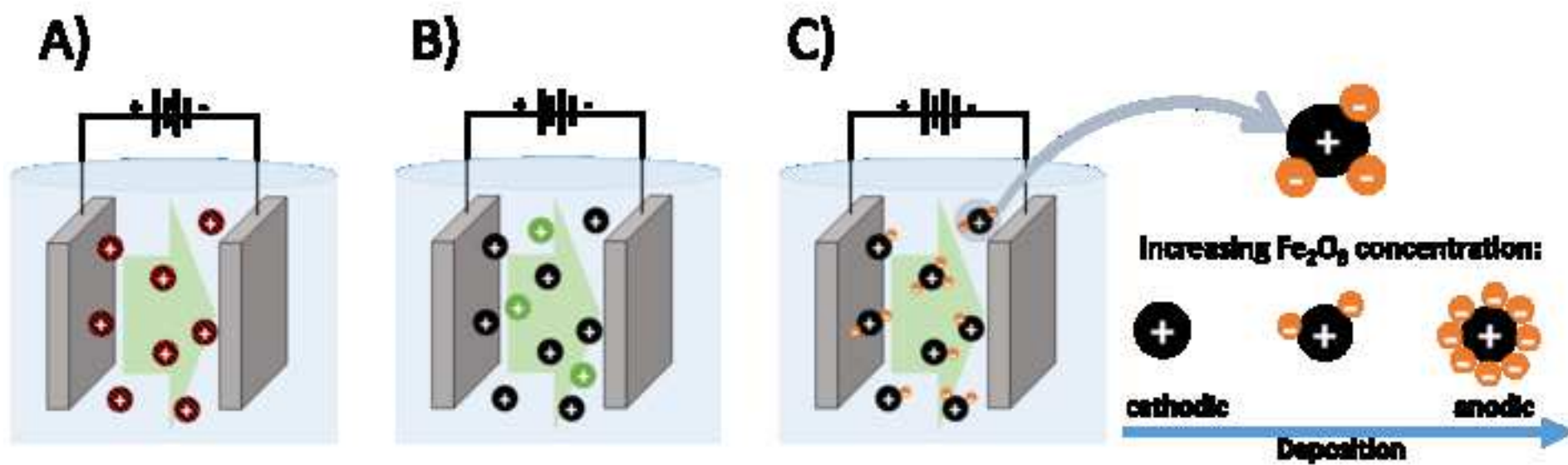


Figure 2  
[Click here to download high resolution image](#)

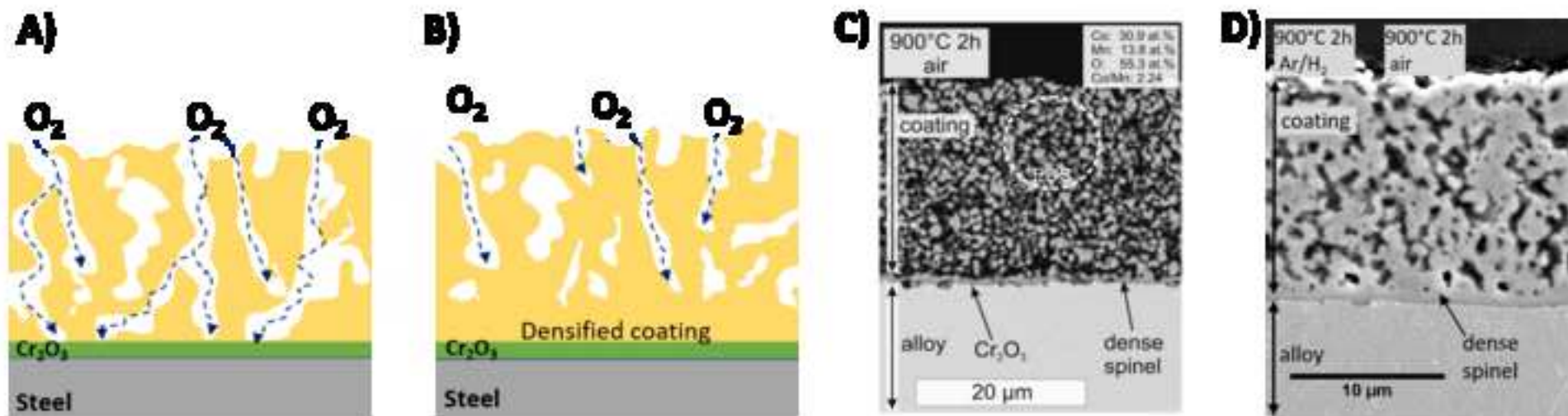




Figure 3  
[Click here to download high resolution image](#)

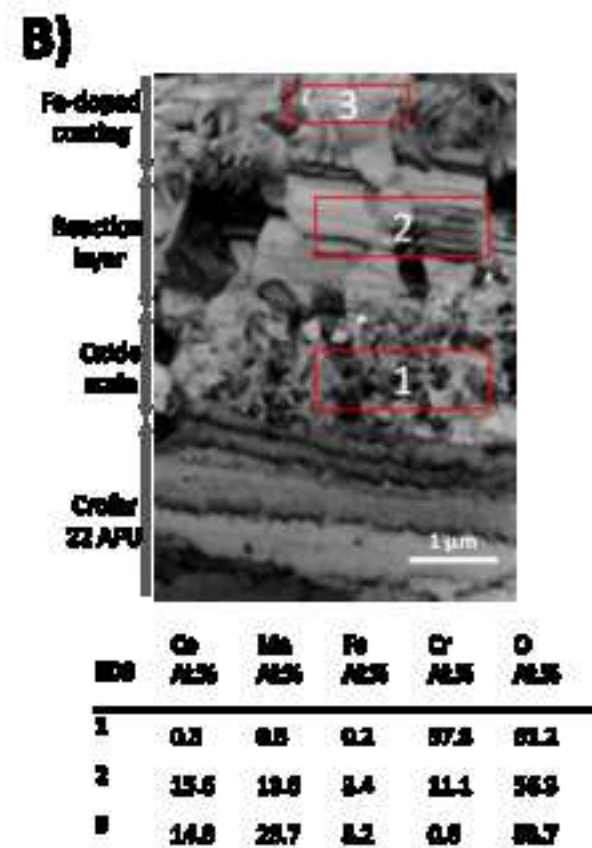
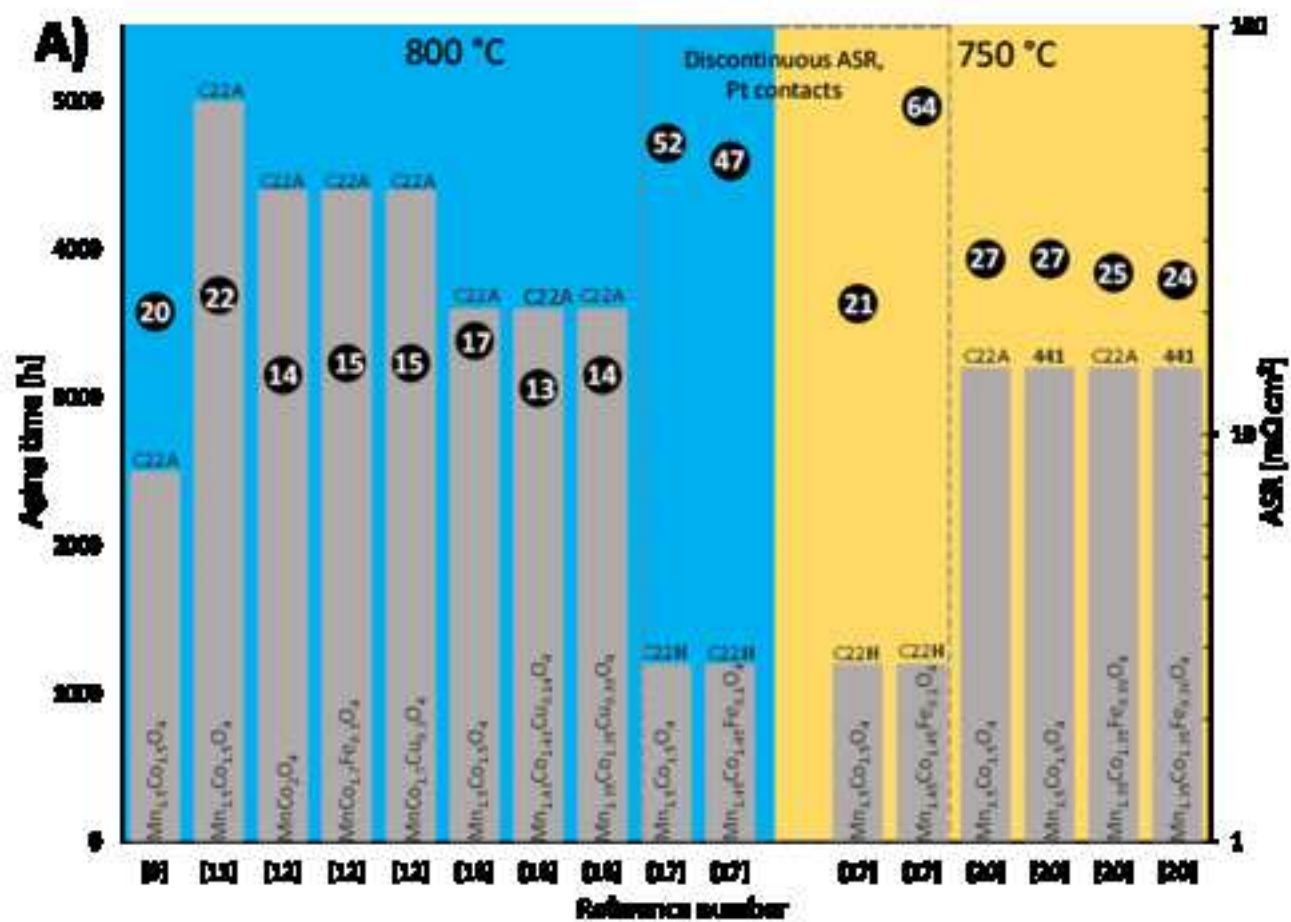


Table 1

Ref.	Year	Spinel Coating Material		Electrophoretic deposition					
		Composition	Synthesis method	Solution [vol%]	Iodine [g/l]	Solid load [g/l]	Voltage [V], time [s]	Electrodes distance [cm]	Substrate
[9]	2015	Mn <sub>1.5</sub> Co <sub>1.5</sub> O <sub>4</sub>	Commercial	60 EtOH 40 H <sub>2</sub> O	-	37.5	5-50 V 5-120 s	-	Crofer 22 APU
[10]	2016	MnCo <sub>2</sub> O <sub>4</sub>	Commercial	100 EtOH	0.15	10.0	30-60 V 60-360 s	1	AISI 430
[11]	2017	Mn <sub>1.5</sub> Co <sub>1.5</sub> O <sub>4</sub>	Commercial	60 EtOH 40 H <sub>2</sub> O	-	37.5	50 V 20s	1	Crofer 22 APU
[12,13]	2017	MnCo <sub>2</sub> O <sub>4</sub> MnCo <sub>1.7</sub> Fe <sub>0.3</sub> O <sub>4</sub> MnCo <sub>1.7</sub> Cu <sub>0.3</sub> O <sub>4</sub>	Spray pyrolysis	50 EtOH 50 IPA	-	39.4	35 V 40-100 s	1.5	Crofer 22 APU
[14]	2018	MnCo <sub>2</sub> O <sub>4</sub>	Commercial	50 EtOH 50 IPA	0.50	7.9	60 V 60 s	-	Crofer 22 APU
[15,16]	2018 2019	Mn <sub>1.5</sub> Co <sub>1.5</sub> O <sub>4</sub> Mn <sub>1.43</sub> Co <sub>1.43</sub> Cu <sub>0.14</sub> O <sub>4</sub> Mn <sub>1.35</sub> Co <sub>1.35</sub> Cu <sub>0.30</sub> O <sub>4</sub>	Commercial Mn <sub>1.5</sub> Co <sub>1.5</sub> O <sub>4</sub> and CuO	60 EtOH 40 H <sub>2</sub> O	-	37.5	50 V 20 s	1	Crofer 22 APU
[17]	2019	Mn <sub>1.5</sub> Co <sub>1.5</sub> O <sub>4</sub> Mn <sub>1.45</sub> Co <sub>1.45</sub> Fe <sub>0.1</sub> O <sub>4</sub>	EDTA	80 Acet 20 IPA	0.50	10	60 V 30 s	1	Crofer 22 H
[18]	2019	Mn <sub>1.5</sub> Co <sub>1.5</sub> O <sub>4</sub>	Commercial	50 EtOH 50 IPA	0.50	15.8	60 V 60 s	-	Crofer 22 APU
[19,20]	2019 2020	Mn <sub>1.5</sub> Co <sub>1.5</sub> O <sub>4</sub> Mn <sub>1.43</sub> Co <sub>1.43</sub> Fe <sub>0.14</sub> O <sub>4</sub> Mn <sub>1.35</sub> Co <sub>1.35</sub> Fe <sub>0.30</sub> O <sub>4</sub>	Commercial Mn <sub>1.5</sub> Co <sub>1.5</sub> O <sub>4</sub> and Fe <sub>2</sub> O <sub>3</sub>	60 EtOH 40 H <sub>2</sub> O	-	37.5	50 V 20 s	1	Crofer 22 APU AISI 441
[21]	2020	MnCo <sub>2</sub> O <sub>4</sub>	Commercial	50 EtOH 50 IPA	0.50	15.8	60 V 60 s	1.5	Crofer 22 H AISI 441 AISI430
[22]	2020	Mn <sub>1.4</sub> Co <sub>1.4</sub> Cu <sub>0.2</sub> O <sub>4</sub>	Commercial	50 IPA 50 ACAC	-	10	40-140 V 2-10 min	-	SUS430
[23]	2017	Cu <sub>1.3</sub> Mn <sub>1.7</sub> O <sub>4</sub>	GNP	75 ACE 25 EtOH	1.09	9	20 V 10 min	1.5	Crofer 22 APU
[24,25]	2018	CuMn <sub>1.8</sub> O <sub>4</sub>	GNP	75 ACE 25 EtOH	1.09	9	20 V 10 min	-	Crofer 22 APU Crofer 22 H
[26]	2019	CuMn <sub>1.8</sub> O <sub>4</sub> Cu <sub>0.6</sub> Ni <sub>0.4</sub> Mn <sub>2</sub> O <sub>4</sub>	GNP	75 ACE 25 EtOH	1.09	9	20 V 10 min	-	Crofer 22 APU

Table 2

	REF	Sintering parameters			
		Type	Temperature [°C]	Time [h]	Atmosphere
Manganese cobalt spinel	[9]	Oxidizing	800, 1000, 1100	2	Static air
	[10]	Oxidizing	1050	1	Static air
	[11]	Oxidizing	1000	2	Static air
	[12]	Two-step	- 900	2	N <sub>2</sub> /H <sub>2</sub> (9 vol.%)
			- 800	2	Static air
	[13]	Oxidizing	900	2	Static air
		Two-step	- 900, 1100	2 - 5	N <sub>2</sub> /H <sub>2</sub> (9 vol.%)
			- 800	2 - 5	Static air
	[14]	Oxidizing	900, 1000, 1100	2	Static air
		Two-step	- 900, 1000, 1100	2	Ar/H <sub>2</sub> (9 vol.%)
			- 900	2	Static air
	[15,16]	Two-step	- 900	2	Ar/H <sub>2</sub> (4 vol.%)
			- 900	2	Static air
	[17]	Two-step	- 900	2	Ar/H <sub>2</sub> (9 vol.%)
			- 900	4	Static air
	[19,20]	Two-step	- 900, 1000	2	Ar/H <sub>2</sub> (4 vol.%)
- 900			2	Static air	
[21]	Oxidizing	900	2	Static air	
	Oxidizing	800	4	Static air	
[22]	Two-step	-800	2	Ar/H <sub>2</sub> (5 vol.%)	
		-750	2	Static air	
Manganese copper spinel	[23]	Two-step	-850*	1	Ar/H <sub>2</sub> (2 vol.%)
			-850*	100	Static air
	[24–26]	Two-step	-1000	12 - 24	Ar/H <sub>2</sub> (2 vol.%)
-850			100	Static air	

\*Uniaxial pressure (from 10 to 100ksi) was applied before the heat treatment

**Declaration of interests**

The authors declare that they have no known competing financial interests or personal relationships that could have appeared to influence the work reported in this paper.

The authors declare the following financial interests/personal relationships which may be considered as potential competing interests: